NON INVASIVE ESTIMATION OF BLOOD UREA CONCENTRATION USING NEAR INFRARED SPECTROSCOPY

Swathi Ramasahayam[1] and Shubhajit Roy Chowdhury[2]

[1]Center for VLSI and Embedded System Technology, IIIT-Hyderabad India,

[2]School of computing and electrical engineering, IITMandi, India

Emails: swathi.ramasahayam@research.iiit.ac.in , src@iitmandi.ac.in

Abstract- ***This paper details about the noninvasive estimation of Urea concentration in blood using near infrared spectroscopy (NIRS) and Artificial neural network based prediction model. The absorption spectrum of the urea has been studied experimentally in order to choose the wavelengths of peak absorption. For this purpose, IR absorption spectrum of 0.1M aqueous urea solution has been collected and analyzed in second overtone region of the near-infra red spectra using the Bruker tensor 27 FTIR spectrometer. Based on the theoretical analysis the optimal wavelength of sensor is found to be 995nm for obtaining proper Photo plethysmograph (PPG). The regression analysis has been carried out on PPG signal with the artificial neural networks for obtaining a prediction model for estimating the blood urea concentration. The mean square error of prediction is found to be ± 2.23mg/dL.***

Index terms*: Noninvasive, blood urea, photo plethysmograph, artificial neural network.**

I.   INTRODUCTION

Estimating the concentration of urea in blood is generally used for diagnosis of renal failure. The level of urea in blood increases as kidney function worsens, which leads to other heart diseases [1]. Currently the traditional lab methods used for monitoring blood urea are invasive in nature and take more processing time to predict the concentration. But more frequent monitoring of blood urea is needed for identifying acute renal failure.

In order to overcome the disadvantages of the invasive methods some noninvasive methods like Raman spectroscopy, vibrational spectroscopy and polarimetric method. However they have the disadvantages like heavy, delicate and expensive instruments [2, 3]. Photoplethysmography is the one of the noninvasive technique being used for estimating the concentration of blood analytes [4]. The spectroscopic analysis is normally carried out at mid infra-red and first overtone regions of the spectrum, where the absorbance of the urea is high. The disadvantage of these regions is that the component cost is very high and the absorption due to other components like water and scattering in fatty tissue. Several attempts have been made for non-invasive estimation of urea concentration like non-invasive estimation based on Reverse iontophoresis [5] and estimating during hemodialysis by employ the optical sensing in the visible range [6-8]. A model has been developed for blood urea monitoring system for the closed loop control of dialysis [9]. Determining the blood urea nitrogen in small specimens by Automatic colorimetric analysis has been described by Helmut J. Richter in [10]. Several other methods have been proposed for estimating blood urea [11, 12]

The current research aims at the estimation of the proper wavelength for urea using near infrared spectroscopy (NIRS). The NIR region falls in the range from 780-2500nm mainly consisting of weak transitions that correspond to combinations and overtones of the vibrational modes observed in mid infrared region. NIRS is a spectroscopic method based on molecular overtones and the combination vibrations of C-H, O-H, and N-H bonds. These combination bands arise from combining C-H, O-H and N-H stretches with other fundamental vibrations. The wavelength of the peak absorption for urea is first theoretically calculated based on the molecular composition. Urea has strong absorbance at the N-H deformation overtone which falls at 2070nm, but the disadvantage with this wavelength of absorption is that the cost of the optode pair is very high. So the attempt has been made to consider the higher overtones based on the

relative absorbance. We have carried out an experiment on aqueous urea using FTIR spectrometer for finalizing the wavelengths for sensor. After which an LED and a photodiode comprising of optode pair is used to justify whether the wavelength of monitoring identified correlates with the theoretical analysis. The PPG obtained from the analog front end circuit is given to artificial neural network for regression analysis and a predictive

II.   THEORITICAL ANALYSIS

a. Visualize bonds between atoms as springs

The classical physics considers the atoms as particles with a given mass in the IR absorption process, and the vibrations of diatomic molecule as shown in figure 1.
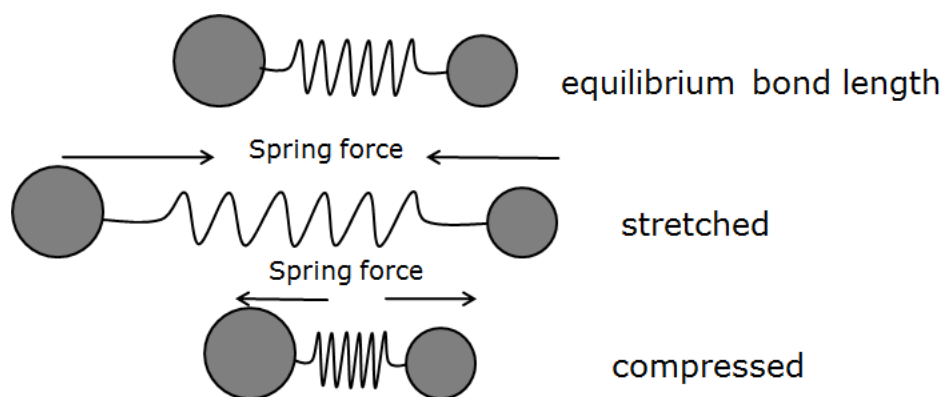
Figure 1. Visualizing bonds as springs

When a photon is incident on a molecule, there will be bond deformations or bond vibrations at different energy levels related to different bonds, depending on the energy of incident photon [13]. So, only the photon with energy that corresponds to the difference between two of its energy levels can be absorbed. The frequency of the vibration is given by the

$$v = 1/2\pi \ (\sqrt{k/m})$$

Where 'k' is the bond strength and 'm' is the reduced mass.

For a urea molecule, the molecular structure is as shown in Fig2.

Table 1 shows the frequencies corresponding to different bond vibrations in urea molecule [14].
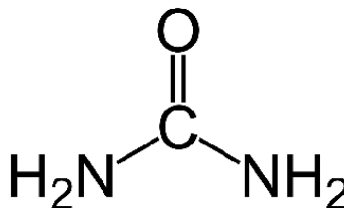
Figure 2. Molecular structure of urea molecule.

Table 1. Fundamental and overtones of urea

Wavelength(nm)	Bond
1160	C=O fourth overtone
1460	Symmetric N-H stretch first overtone
1520	N-H stretch first overtone
1990	N-H stretch/N-H bend combination
2030	C==O stretch second overtone
2070	N-H deformation overtone

At a deeper level absorption of light can be seen as dependent on the probability of absorbance of a photon by the molecule. For nth overtone final energy is (n+1)*E, where E is the fundamental energy. As n increases, probability of absorbance decrease rapidly and hence intensities of absorbance decrease as overtones increase. The absorption at fundamental frequency is calculated and from that the absorption at second overtone is calculated relatively [15].

b. Wavelength selection based on peak absorption

The absorption spectrum of the urea has been studied in order to choose the wavelengths for LEDs. For this purpose an IR absorption spectrum of 0.1M aqueous urea solution has been collected and analyzed in second overtone region of the near-infra red spectra using the Bruker tensor 27 FTIR spectrometer. Fig.3 shows the absorption spectrum of the urea over the second overtone region. From the spectra obtained the optimal wavelength where the absorption is considered suitable for urea extraction. We can observe that the absorption peaks in this region are very narrow typically of the order of the 2nm to 5nm but the LED emits the light over a range

of wavelengths. The wavelengths are chosen such that the weighted average of the absorption over the spectral bandwidth of the LED is high. While calculating this weighted average the intensity of light emitted by the LED acts as weight for the absorption at that particular wavelength.
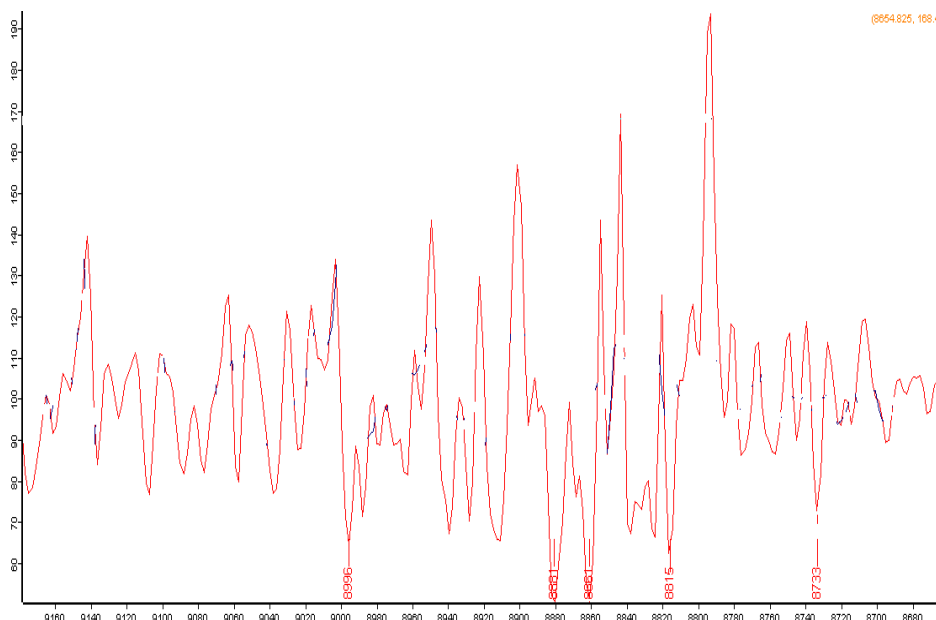
Figure 3. Absorption spectrum of urea over NIR region

In order to verify whether the theoretical results obtained based on the molecular composition of urea are matching with the experimental results. We have conducted the experiments with FTIR spectrometer to get the IR spectrum of the aqueous urea and analyzed the spectrum to get the wavelength in the range of 750 to 1100nm and it is found that 995nm is an appropriate wavelength for studying the characteristics of urea.

In order to justify the results obtained an experiment is carried out with optical components like LED and photodiode comprising an optode pair which is discussed in the below section.

III.   PPG SENSING CIRCUIT

a. Photoplethysmography (PPG) using optode pair

Photoplethysmography is an optical technique widely used to measure the pulse rate, arterial blood oxygen saturation and blood volume changes. It uses a clip which contains a light source and a detector on the opposite sides to detect the cardio vascular pulse wave that propagates

through the body. The PPG waves can be described as containing a DC component due to venous blood and an AC component due to blood volume changes in the arteries.

According to Beer-lambert's law the absorbance of light by a liquid is related to the concentration of the material by

$$A = \epsilon Cl$$

Where the molar absorptivity of solute at a particular wavelength, C is the concentration of the solute and is the path length.

From this we can say that if the intensity (Peak to peak value) of the PPG is high then the absorbance of the chromophore is high in that region, which is in turn directly proportional to the concentration of the chromophore. Figure 4 shows the basic PPG waveform with different components.
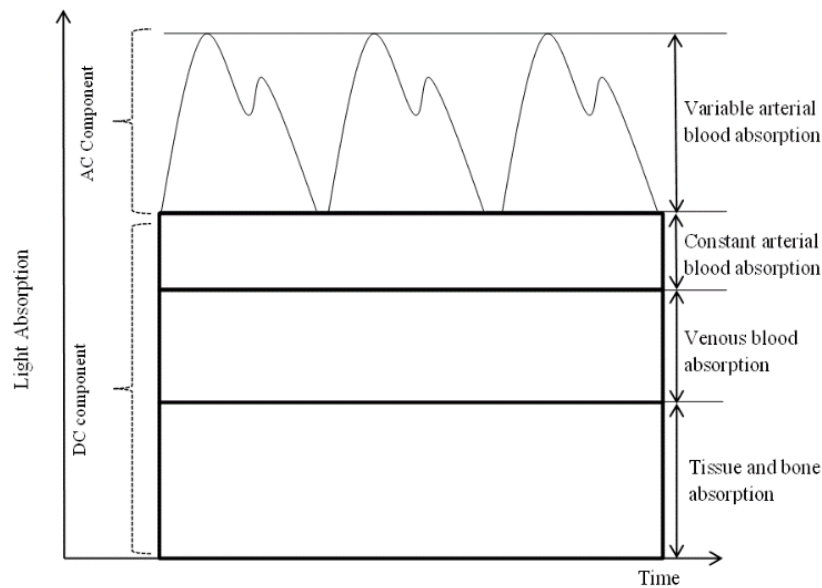
Figure 4. Photo plethysmograph with various components

A. Testing using optode pair

As discussed in the previous section, the wavelength of peak absorption for urea has been chosen to 995nm.The block diagram of the experimental set up for getting PPG is shown in the Figure 5.
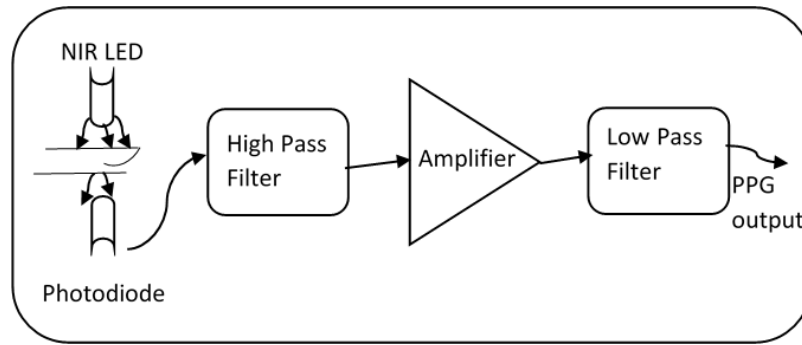
Figure 5. PPG sensing circuit

It consists of the finger clip with LED acting as a light sensor and the photodiode as the detector to detect the small changes in the incident light as it passes through the finger. This light is converted in to an equivalent current by the detector and is high pass filtered with a cut off frequency of 0.8Hz. Then it is given to the trans-impedance amplifier for amplification of the signal. After this the signal is low-pass filtered to get the required PPG which is mainly because of the urea. The cut off frequency for low pass filter is 10Hz.

B. Trans-impedance Amplifier

The trans-impedance amplifier is used to convert the current from the photodetector into voltage i.e. I to V converter which is built using an operational amplifier. The trans-impedance amplifier also provides gain to the PPG signal.
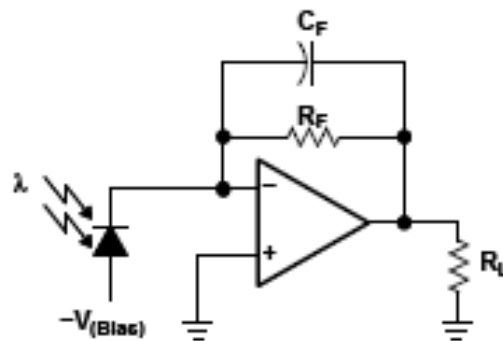
Figure 6. Trans-impedance Amplifier

The first part of the photodiode receiver is a trans-impedance amplifier. The purpose of this is to take the small current (μA) supplied by the photodiode and amplify the impedance of this signal. This gives the signal a voltage that is useful for further processing and decoding. It is simply an

operational amplifier with a feedback resistance and a feedback capacitance. The operational amplifier used was the Texas Instruments wide-band FET input operational amplifier. A FET input op amp was necessary because it can operate with a low input current bias, usually in the nA range. A BJT input op amp requires an input current in the mA range.

Trans-impedance amplifiers are generally operated at a very high gain. This produces a strong tendency for the amplifier to go into oscillation at high frequencies above the gain bandwidth product. This problem can be eliminated by adding a capacitor in the feedback loop, which lowers the gain at very high frequencies.

C. High Pass Filter

The high pass filter in the circuit diagram is used to remove the DC component in the PPG obtained. Because of the DC component, the PPG is at a value higher than the ground. Our signal of interest is only the AC component which is obtained by passing through high pass filter. In this case, we have assumed that the cutoff frequency should be 0.8 Hz. We used a passive high pass filter which is constructed by using resistor and capacitor and the output is given to the input of 4th order active low pass filter which is constructed using operational amplifier (LM741).
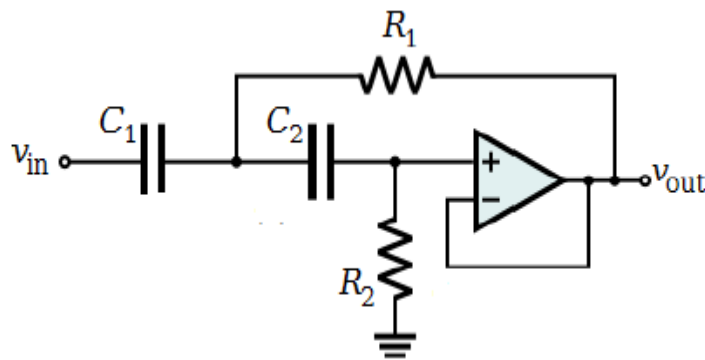
Figure 7. High Pass Filter

D. Low Pass Filter

The low pass filter is constructed using two operational amplifier and resistors and capacitors. The 4th order low pass filter is constructed by cascading two 2nd order low pass filters. Since we

are constructing real time filters, the filter would be having a pass band and a stop band. The stop band would be steeper if the order of the filter is high. The Q factor also decides the smoothness of the filter. We used this low pass filter to basically remove the power line signal (50Hz) which would otherwise interfere with the PPG and would give us wrong results. We decided that the cutoff frequency for this low pass filter would be 10. The circuit of the low pass filter is as shown in figure. 8.
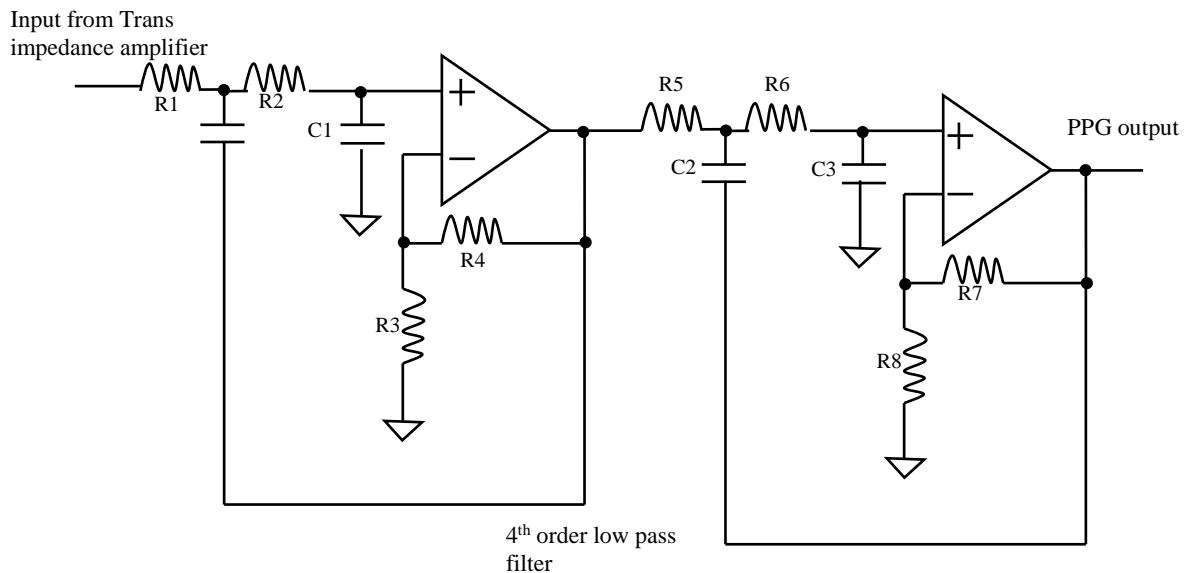
Figure 8. Low Pass Filter

The formula for cutoff frequency is:

$$f_c = 1/2\pi RC$$

After calculations by plugging in fc=10Hz and π=3.14, I chose C=100nF and obtained R=165k.

The Q factor was chosen to be 1 since the response was straighter.

$$Q=1/ (3-A)$$

By plugging in Q=1, we obtain A=2 where A is the gain of the amplifier.

The gain of a non-inverting amplifier is:

$$A=1+ (R2/R3)$$

Since A=2, we obtain R2/R3=1, therefore I chose R2=R3=1k.

The output of the low pass filter is given to an oscilloscope to view a PPG signal which is shown in Figure. 9
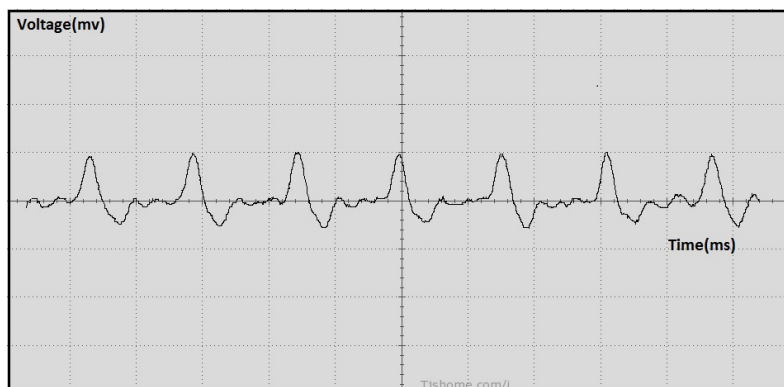
Figure 9. PPG waveform

From the above figure we can infer that the PPG signal with good intensity signifies that the wavelength identified for estimation of urea in blood is appropriate.

IV.   CALIBRATION OF OPTICAL MEASUREMENTS USING ARTIFICIAL NEURAL NETWORKS

In order to estimate the urea concentration from the Photo plethysmograph (PPG) readings, Calibration has to be carried out on a measured set of optical readings (PPG) and corresponding urea concentrations to develop a model which will allow prediction of urea concentration in future.

Many attempts have been made based on univariate regression analysis for single wavelength prediction of blood analytes (16, 17). The biological data is more complex due to the presence of several components whose spectral features overlap.

PLS and PCR are the most widely used chemo-metric techniques for quantitative analysis of complex multicomponent mixtures. These methods are not optimal when the relationship between the IR absorbance's and the constituent concentration deviates from linearity. The theory and the application of Artificial Neural networks (ANN) in modeling chemical data have been widely presented in the literature [18, 19].

a. Artificial neural networks

Neural networks are typically organized in layers, each layer consists of interconnected nodes with neurons. The basic feed forward structure is made up of input layer, one or more hidden layer and the output layer. Patterns are presented to the network via the input layer, which communicates to one or more hidden layers where the actual processing is done via a system of weighted connections from the neurons in the hidden layer.

Learning rule is used to modify the weights of all the interconnected neurons in each layer based on the input patterns that it is presented with. Although there are many different kind of learning rules used by the neural networks. Delta rule is one of such kind which is generally used by common class of artificial neural networks called backpropagation neural network.

With the delta rule, as with other types of backpropagation, learning is supervised process that occurs with each cycle or epoch through a forward activation flow of outputs and backwards error propagation of weight adjustments.
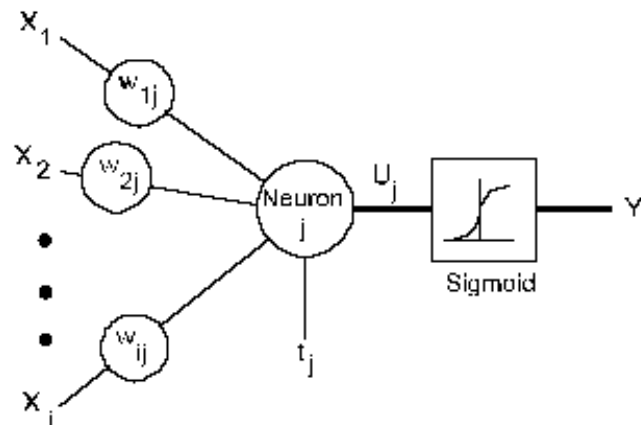
Figure 10. Structure of single neuron

Initially the neural network randomly guesses the output based on the given input pattern and then it compares how far the output is from the actual value and makes an appropriate adjustment to its connection weights. Within each hidden layer there is a sigmoidal activation function which polarizes network activity and helps it to stabilize.

a.   Structure of the feed forward network

There are different types of neural network models based on the type of architecture, learning algorithm, and activation function. Here we have used a network comprising of two layers viz., hidden layer and the output layer as shown in Fig.11. The hidden layer has 10 hidden neurons and the output has only one neuron. In the hidden layer the weighted sum of inputs with the sigmoid activation function (fs) are processed. The output layer has single neuron with linear activation function of where the weighted sum of outputs of the hidden layer with linear activation function are processed to give the final output of the network.
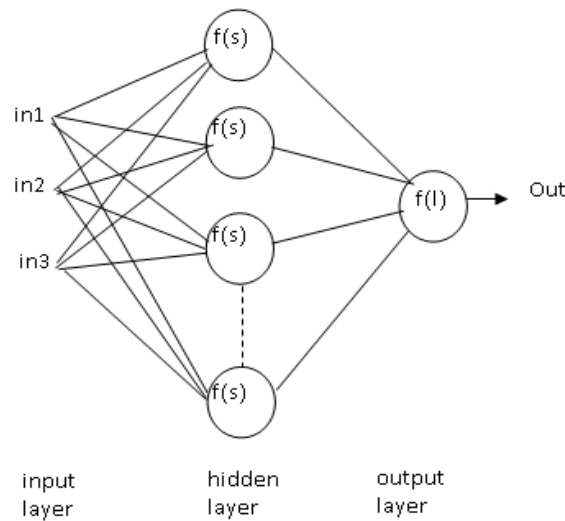
Figure 11. Structure feed forward neural network

The optical densities for various subjects has been calculated based on the equation (5) from the PPG output of front end analog circuit. These optical densities are given as inputs to the network and the invasive urea values as targets to train the network and predict the near future values of urea. During first stage which is the initialization of weights, some small random values are assigned. During feed forward stage each input unit receives an input signal and transmits this signal with a weightage to each of the hidden neurons. Each hidden unit summarizes the inputs and its bias (b), then calculates the activation function (fs) and sends its signal to each output unit. The output unit calculates the activation function (fl) with bias to form the response of the net for the given input pattern. [20]

V.   REGRESSION RESULTS

In this current work, ANN has been used for function fitting to develop a model based on the PPG data and invasive urea measurements. The optical densities are given as input to train the feed forward neural network for estimating the concentration of urea.

The performance of the regression analysis was evaluated in terms of root mean square error of prediction for the training data and is given by Eq. (9)

$$RMSE_1 = \sqrt{\frac{\sum_{i=1}^{N1}(x_i - y_i)^2}{N1}}$$

MATLAB is used to design a neural network for predicting the output. Below figure shows the network designed in MATLAB using neural network tool.
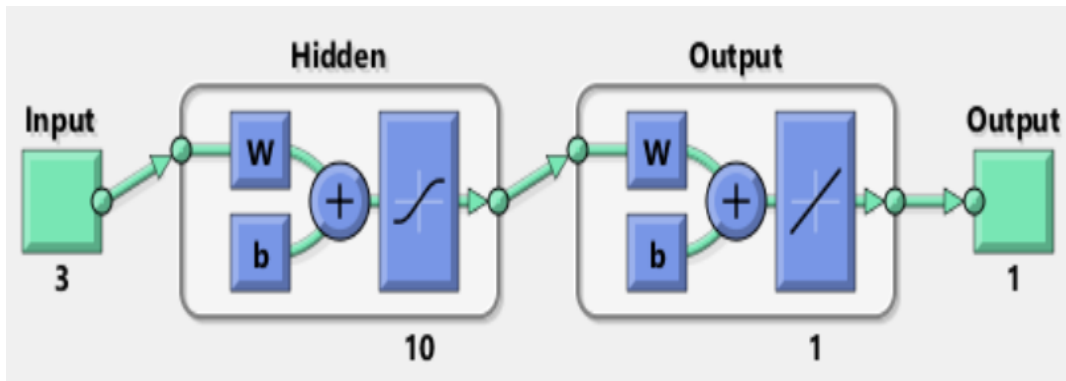
Figure 12. Matlab based neural network model

Clinical trials have been carried out on 30 subjects, based on the invasive and the measured urea values. Results of regression analysis on the input data set are shown in Fig.13 where the parameter R signifies the correlation between estimated urea and the actual urea levels, we can observe that R is nearly equal to 1 for training, validation and test. For this a root mean square error of 2.23mg/dL is obtained. Fig.14 signifies the performance of the neural network, it details about the mean square error (MSE) versus the number of epochs. It tells us about the variation in the MSE for training, test and validation data while training for certain number of epochs. Similarly the Fig.15 and16 indicate about the training states and the error histogram respectively.
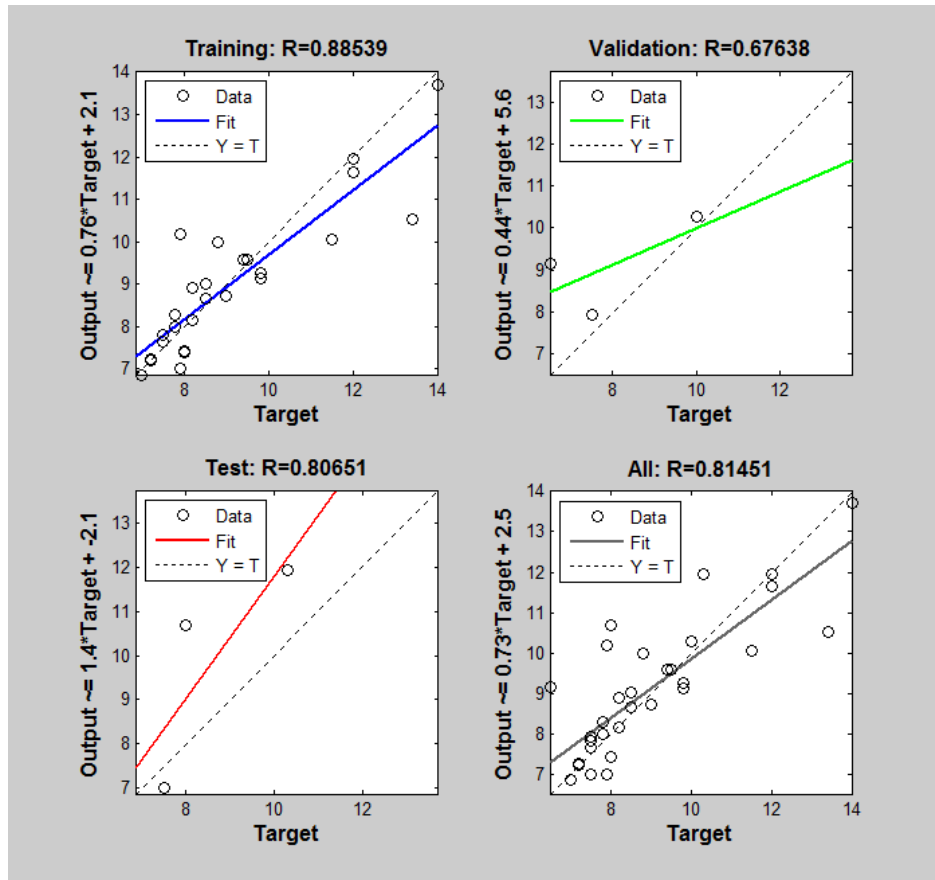
Figure 13. Training, testing and validation results showing the regression factor
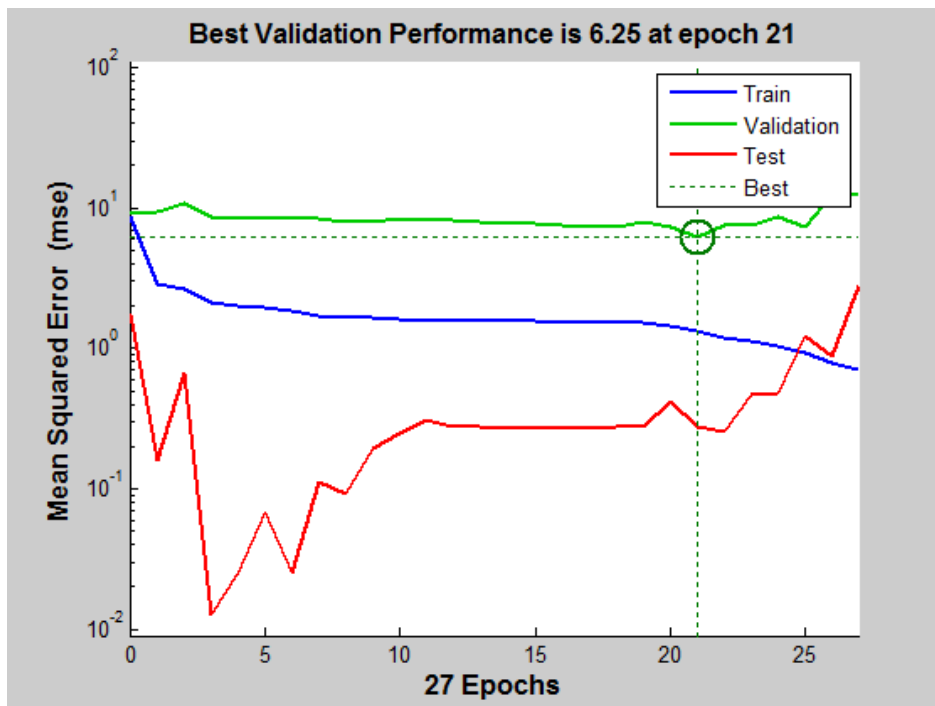
Figure 14. Performance graph for Training, testing and validation data
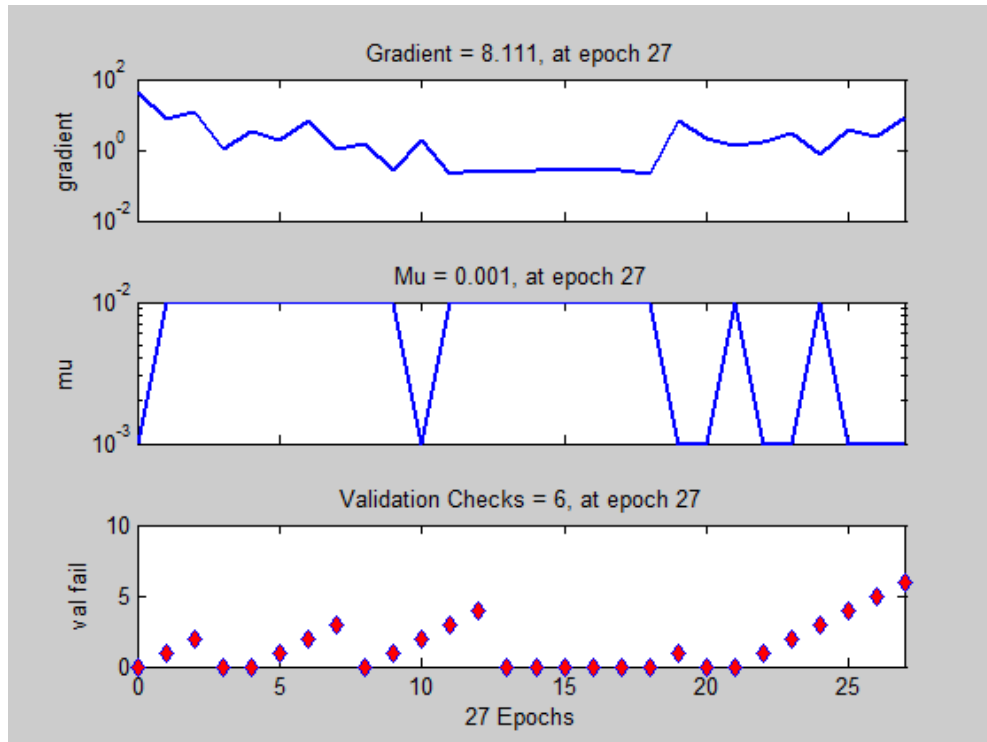
Figure 15. Training state of the neural network
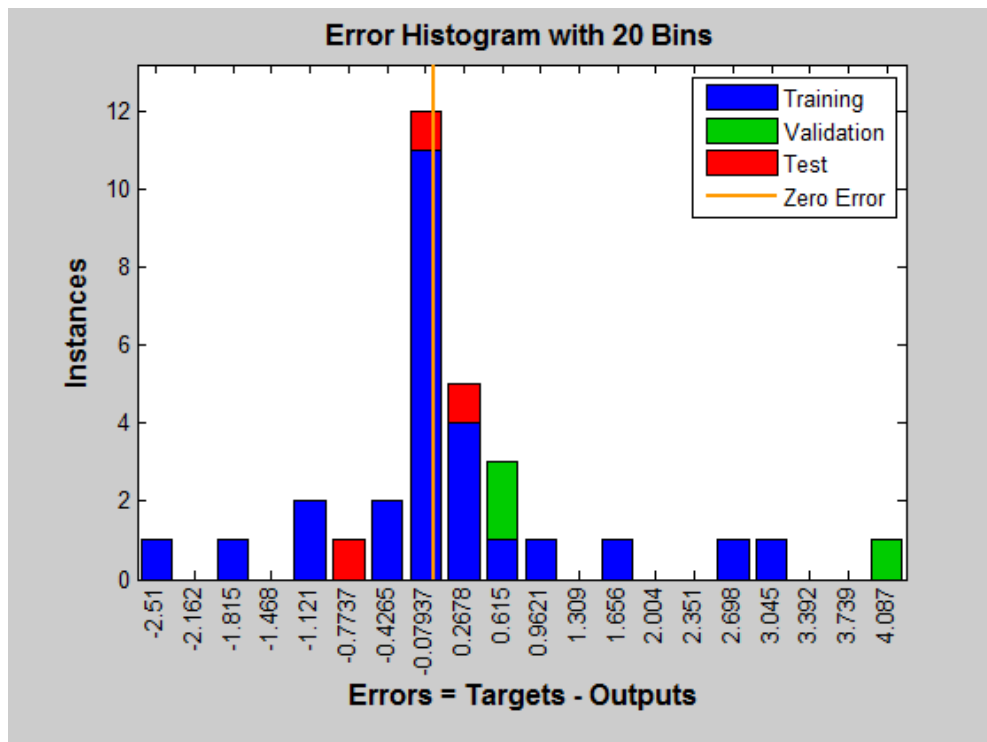
Figure 16. Error Histogram

Clinical trials has been carried out on 50 patients conforming to the declaration of Helsinki using the proposed blood urea monitoring system and the results are compared with the invasive lab test results.

Let p be the number of patients who has their blood urea levels above normal range, q be the number of patients with blood urea levels are under normal range but the test shows the results above the normal range, r be the number of patients where the test shows the results below the normal range, but they have the levels above normal range, s be the number of patients where the test shows the results below the normal range, and they are below the normal range. In our case, for the population of patients being sampled, p=37, q=2, r=5, s=6.

The prevalence of disease is given by

$$Pr = \frac{(p+r)}{(p+q+r+s)} = 0.84$$

Sensitivity of diagnosis,

$$Se = \frac{p}{(p+r)} = 0.880$$

Specificity of diagnosis,

$$Sp = \frac{s}{(q+s)} = 0.75$$

False positive,

$$1 - Sp = \frac{q}{(q+s)} = 0.25$$

False negative,

$$1 - Se = \frac{r}{(p+r)} = 0.1191$$

Accuracy of diagnosis is given by,

$$\frac{(p+s)}{(p+q+r+s)} * 100\% = 0.86$$

Table. 5 Comparative study showing the accuracy of the diagnosis by varying the neurons in hidden layer

No. of hidden neurons	p	q	r	s	Se	Sp	Accuracy
10	37	2	5	6	0.904	0.75	0.86
11	37	3	4	6	0.904	0.75	0.86
12	39	2	3	6	0.928	0.75	0.90
13	39	2	3	6	0.928	0.75	0.90
14	40	1	2	7	0.952	0.87	0.94
15	40	1	2	7	0.952	0.87	0.94

In order to investigate, whether the number of neurons in the hidden layer have an impact on the accuracy of monitoring, the number of neurons in the hidden layer in the neural network has been varied and the testing accuracy is ascertained. A test carried out using the proposed system is considered to be accurate, as the results obtained are with the proposed system agrees with the conventional pathological lab test results within an error window of.

Table 5 shows the effect of varying the number of neurons in the hidden layer on the accuracy and other statistics. This analysis indicates that as the number of hidden neurons are increased, the accuracy of the diagnosis is increased which is due to increased computational accuracy in neural network. We can see that the maximum achievable accuracy using 15 neurons is 94%.

VI.   CONCLUSION

In the current work, we have designed a noninvasive, low cost, and sensitive and user friendly device for blood urea measurement based on a near infra-red spectroscopy and the artificial neural networks. The LED and the Photodetector are chosen according to the wavelength obtained from the theoretical analysis and the experiment is carried out to find that the output obtained is of high intensity which shows high correlation between theoretical and experimental results.

Artificial neural network has been employed for regression analysis on PPG data and obtain a prediction model. The neural network based prediction model is used to estimate the future values of blood urea based on the PPG output obtained from selected near infra-red sensors. Accuracy of the prediction model is found to be 2.23mg/dL. The sensitivity, specificity and the accuracy of the model has been derived and the accuracy is found to be 86%. The effect of number of hidden neurons in the hidden layer on the sensitivity specificity and accuracy of the prediction model has been analyzed. The Accuracy of the system can also be improved by increasing the input data set to the neural network model.

REFERENCES

[1] H.M. Heise, in: R.A. Meyers (Ed.), Encyclopedia of Analytical Chemistry, vol. 1, John Wiley Press, New York, 2000, pp.1-27

[2] J.P. Wicksted, R.J. Erckens, M. Motamedi, W.F. "Raman Spectroscopy studies of metabolic concentrations in aqueous solutions and aqueous humor specimens March, Appl. Spectrosc. 49(7) (1995) 987–993

[3] S.J. Alcock , B. Danieslson , A.P.F. Turner, "Advances in the use of *in vivo* sensors", Biosensors and Bioelectronics Volume 7, Issue 4, 1992, Pages 243-254

[4] John Allen, "Photoplethysmography and its application in clinical physiological measurement" Published 20 February 2007 • 2007 IOP Publishing Ltd • Physiological Measurement Mar; 28(3):R1-39.

[5] Wascotte V1, Rozet E, Salvaterra A, Hubert P, Jadoul M, Guy RH, Préat V "Non-invasive diagnosis and monitoring of chronic kidney disease by reverse iontophoresis of urea in vivo", Eur J Pharm Biopharm. 2008 Aug; 69(3):1077-82. doi: 10.1016/j.ejpb.2008.02.012. Epub 2008 Feb 20

[6] G. A. Martinez, "Measurement of Blood Urea Based in Optical Sensing by Employ in Hemodialysis Treatment," *Engineering in Medicine and Biology Society, 2006. EMBS '06. 28th Annual International Conference of the IEEE*, New York, NY, 2006, pp. 2231-2234.

[7] Martinez, G.A.; Bragos, R., "No invasive Measurement of Urea in Blood Based in Optical Sensing for their Employment in the Hemodialysis Processes.," in Instrumentation and Measurement Technology Conference, 2005. IMTC 2005. Proceedings of the IEEE, vol.2, no., pp.1397-1400, 16-19May 2005 doi: 10.1109/IMTC.2005.1604379

[8] Gustavo Adolfo Martinez, "On-Line Measurement of Blood Urea Based in Optical Sensing by Employ in Hemodialysis Treatment", World Congress on Medical Physics and Biomedical Engineering 2006 Volume 14 of the series IFMBE Proceedings pp 651-655

[9] Smirthwaite PT, Fisher AC, Henderson IA et al. "Development of blood urea monitoring system for the closed loop control of dialysis", ASAIO J. 1993;39; M:342-7

[10] Helmut J. Richter and Yvette S. Lapointe, "A Simple Method for the Determination of Blood Urea Nitrogen, with Special Reference to Automatic Colorimetric Analysis" Clinical ChemistryDecember 1959 vol. 5 no. 6 617-620

[11] Sternby J. Urea Sensors-a world of possibilities. Adv Renal Replace Ther. 1999; 6: 265-72

[12] Jacobs P. Suls J, Sansen W, et al. "A disposable urea sensor for continuous monitoring hemodialysis efficiency", ASAIO J. 1993; 39; M: 353-8

[13] Airat k. amerov, jun chen, and mark a. arnold,"Molar Absorptivities of Glucose and Other Biological Molecules in Aqueous Solutions over the First Overtone and Combination Regions of the Near-InfraredSpectrum".APPLIEDSPECTROSCOPY Vol. 58, Issue 10, pp. 1195-1204 (2004)

[14] Z. Piasek and T. Urbanski, "The infrared absorption spectrum and structure of urea," Bulletin de l'Académie Polonaise des Sciences: Série des Sciences Chimiques, vol. 10, pp. 113–120, 1962.

[15] A. I. Pavlyuchko, E. V. Vasilyev, and L. A. Gribovb, "calculations of molecular ir spectra in the overtone and combination frequency regions", November 2011, Volume 78, Issue 5, pp 639-645.

[16] D. Riordan, P. Doody and J. Walsh, The use of artificial neural networks in the estimation of the perception of sound by the human auditory system, International journal on smart sensing and intelligent systems vol. 8, no. 3, pp 1806-1836, September 2015.

[17] C.PerezGandia, A.Facchinetti, G.sparacino, C.cobelli, E.J.Gomez, M.Rigla, A.deLeiva, M.E.Hernando,"Artificial neural network algorithm for on-line glucose prediction from continuous glucose monitoring", Diabetes Technol.Ther. 2010, 12, 81-88

[18] Robertson G, Lehman D, Sandham, Hamilton, "Blood Glucose Prediction Using Artificial Neural Networks Trained with the AIDA Diabetes Simulator: A Proof-of-Concept Pilot Study", Journal of Electrical and Computer Engineering, 2011, Article ID 681786, 11 pages.

[19] Bhandare, P., Mendelson, Y., Peura, R.A.: Multivariate Determination of Glucose in Whole Blood Using Partial Least-Squares and Artificial Neural Networks Based on Mid-Infrared Spectroscopy. J. Applied Spectroscopy 47, 1214–1221 (1993).

[20] Smits, J.R.M., Malssen, W.J., Buydens, L.M.C., KatemanG. Using Artificial Neural Networks for Solving Chemical Problems. Part 1. Multi-layer Feed-forward Networks. J.Chemometrics and Intelligent Laboratory Systems 22, 165–189 (1994)